

Articles

Preparation and Characterization of 1,3-Butadiene and Isoprene Complexes, $W_2(OCH_2^tBu)_6(diene)(py)$, and Studies of the Selective Hydrogenation of 1,3-Dienes

Jane T. Barry, John C. Bollinger, Malcolm H. Chisholm,* Katherine C. Glasgow, John C. Huffman, Eric A. Lucas, Emil B. Lubkovsky, and William E. Streib

Department of Chemistry and Molecular Structure Center, Indiana University, Bloomington, Indiana, 47405

Received January 29, 1999

In hydrocarbon solutions $W_2(OCH_2^tBu)_6(py)_2$, **1**, and 1,3-butadiene and isoprene reversibly form adducts $W_2(OCH_2^tBu)_6(diene)(py)$, compounds **2** (diene = 1,3-butadiene) and **3** (diene = isoprene). The structures of **1**, **2**, and **3** are reported. For **1** there is a central $O_3NW\equiv WNO_3$ core with $W-W = 2.334(1)$ Å, and each W atom is in a distorted square-based pyramidal environment with the $W=W$ bond in the apical site. In **2** and **3** there is a common $W_2O_6C_4N$ core wherein the diene adopts a novel mode of coordination, μ, η^1, η^4 . One W atom is coordinated to five oxygen atoms and the bridging carbon atom of the μ -diene ligand, while the other is bonded to three oxygen atoms, a pyridine nitrogen, and four carbon atoms of the diene. The structure may be viewed as being derived from a confacial bioctahedron with two bridging OR ligands and one bridging alkyl. In this view the diene can be considered as a μ -metalated π (η^3 -)allyl or a 2- ligand. The $W-W$ distances are 2.471(1) Å in **2** and 2.464(1) Å in **3**, consistent with a $(W=W)^{8+}$ core. The isoprene structure **3** reveals a disorder involving primarily the location of the isoprene C-Me group over two sites. The variable-temperature 1H and $^{13}C\{^1H\}$ NMR spectra reveal the dynamic equilibria involving **1** + the diene and **2** and **3**. The spectra of **2** and **3** are entirely reconcilable with the solid-state structures, and for the deuterated complexes $W_2(OCd_2^tBu)_6(diene)(py)$ all the 1H signals of the diene are assigned by a combination of COSY and HETCOR spectra. For **3** there exists a mixture of the two isomers, differing with respect to the position of the isoprene C-Me group as seen in the solid-state structure. These interconvert by a reversible dissociative pathway. Though other 1,3-dienes have not been found to form adducts, we have found selective 1,2-hydrogenation to give 3-enes in the presence of $W_2(OCH_2^tBu)_6(py)_2$. This hydrogenation is not restricted to dienes but is also observed for cis-cyclic olefins. The addition of D_2 to norbornene reveals the stereospecific cis-addition at the endo sites. The addition of D_2 to 1,3-butadiene and isoprene gives $CH_2DCHDCH=CH_2$ and $CH_2DCHDCMe=CH_2$, respectively. These results are discussed in terms of other substrate activations by $W_2(OR)_6$ compounds and other hydrogenation reactions.

Introduction

$W_2(OR)_6$ compounds provide templates for the uptake of small organic molecules, such as alkynes and olefins, as well as other unsaturated diatomic molecules (CO, NO).¹ The key features underpinning this reactivity are (i) coordinative unsaturation at the ditungsten center and (ii) the redox active $W\equiv W$ bond. $W_2(OR)_6$ compounds may undergo reversible ($R = ^iPr$) or irreversible ($R = CH_2^tBu, CH_2^cBu, CH_2^iPr, CH_2^cPen$) association to give $W_4(OR)_{12}$ compounds.² To suppress this reaction, Lewis bases such as pyridine may be used to trap the

$W_2(OR)_6$ complexes via the facile reversible equilibrium shown in eq 1.



Thus, in solution $W_2(OCH_2^tBu)_6(py)_2$ provides a source of the labile complex $W_2(OCH_2^tBu)_6$, which has previously been shown to activate $C-C^3$ and $C-O$ double bonds⁴ as well as α, β -unsaturated aldehydes and ke-

(1) Chisholm, M. H.; *J. Chem. Soc., Dalton Trans.* **1996**, 1781.

(2) Chisholm, M. H.; Clark, D. L.; Hampden-Smith, M. J. *J. Am. Chem. Soc.* **1989**, *111*, 574.

(3) Chacon, S. T.; Chisholm, M. H.; Eisenstein, O.; Huffman, J. C. *J. Am. Chem. Soc.* **1992**, *114*, 8497.

(4) Chisholm, M. H.; Huffman, J. C.; Lucas, E. A.; Sousa, A.; Streib, W. E. *J. Am. Chem. Soc.* **1992**, *114*, 2710, and references therein.

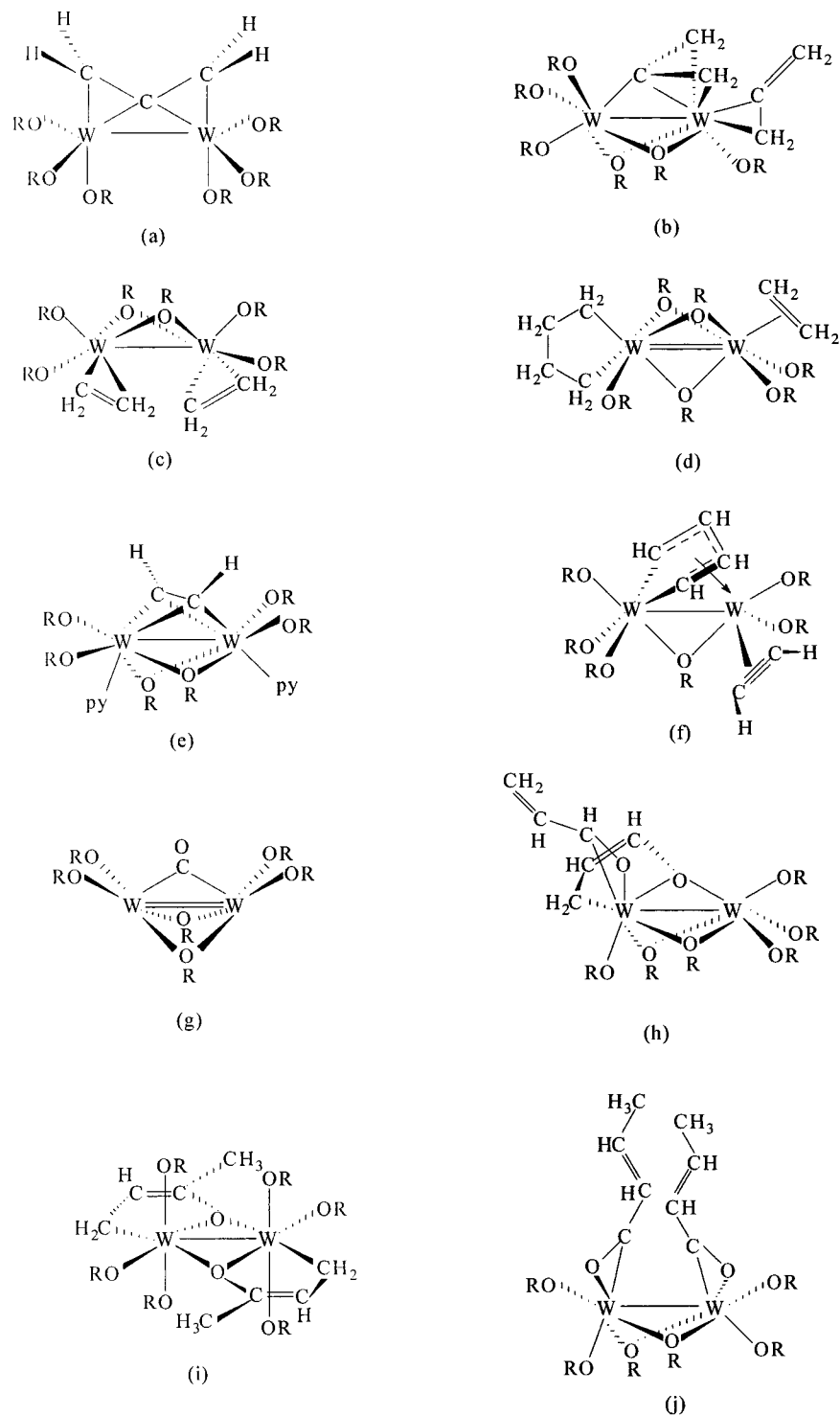


Figure 1. Structural representations of $W_2(OR)_6$ adducts with (a) allene, $R = {}^t\text{Bu}$, (b) $C_3H_4 = \text{allene}$, $R = {}^t\text{Bu}$, (c) ethene, $R = \text{CH}_2{}^t\text{Bu}$, (d) ethene, $R = {}^i\text{Pr}$, (e) ethyne, $R = {}^t\text{Bu}$, (f) ethyne, $R = {}^i\text{Pr}$, (g) CO, $R = {}^t\text{Bu}$, (h) $\text{CH}_2=\text{CH}-\text{CH}=\text{O}$, $R = \text{CH}_2{}^t\text{Bu}$, (i) $\text{CH}_2=\text{CHC}(\text{Me})=\text{O}$, $R = \text{CH}_2{}^t\text{Bu}$, (j) $\text{MeCH}=\text{CHCH}=\text{O}$, $R = \text{CH}_2{}^t\text{Bu}$. [Compounds b and c are formed reversibly in solution.] Details of the structures of these compounds can be found in papers cited in ref 1.

tones.⁵ Several modes of addition have been observed as shown in Figure 1. A question concerning the reactivity of the $W=W$ bond commonly arises: How does

it react with dienes? Can one obtain metalloorganic analogues of the Diels–Alder⁶ reaction? In this paper we address this question, together with an investigation of the hydrogenating properties of these systems. A preliminary report on the formation of the 1,3-butadiene adduct has appeared.⁷

(5) Chisholm, M. H.; Lucas, E. A.; Sousa, A. C.; Huffman, J. C., *J. Chem. Soc., Chem. Commun.* **1991**, 847.

(6) (a) Diels, O.; Alder, K. *Justus Liebigs Ann. Chem.* **1928**, 460, 98. (b) For a general review see: *Advanced Organic Chemistry, Part B: Reactions and Synthesis*, 3rd ed.; Carey, F. A., Sundberg, R. J., Eds.; Plenum Press: New York, 1990; Chapter 6, and references therein.

(7) Chisholm, M. H.; Huffman, J. C.; Lucas, E. A.; Lubkovsky, E. B. *Organometallics* **1991**, 10, 3424.

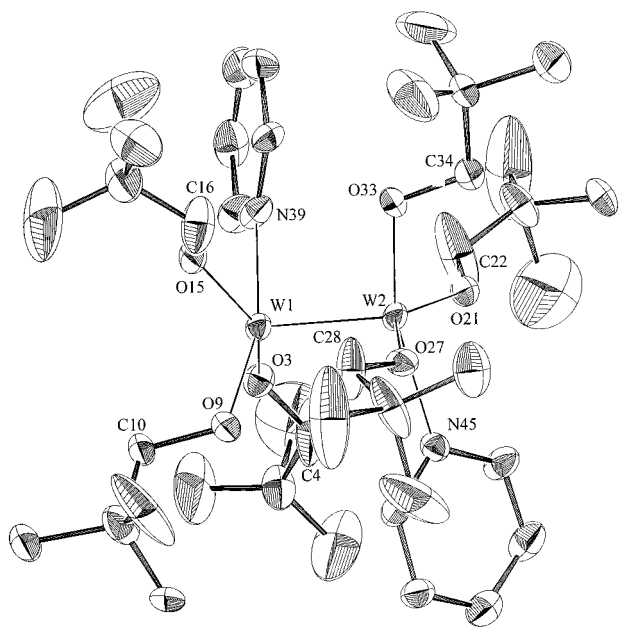


Figure 2. Structure of $W_2(OCH_2^tBu)_6(py)_2$, **1**. Thermal ellipsoids are shown at the 50% probability level.

Results and Discussion

Preparation of Diene Adducts, $W_2(OCH_2^tBu)_6(1,3\text{-butadiene})(py)$, **2, and $W_2(OCH_2^tBu)_6(\text{isoprene})(py)$, **3**.** In toluene solutions $W_2(OCH_2^tBu)_6(py)_2$ reacts with 1,3-butadiene and isoprene to give dark blue or purple solutions from which crystals of both **2** and **3** have been obtained upon cooling ($-20\text{ }^\circ\text{C}$) of the mother liquor. The compounds are thermally unstable and lose the diene at room temperature under a nitrogen atmosphere. They are also hydrolytically sensitive, which has made their handling problematic. However, they are kinetically persistent at $-20\text{ }^\circ\text{C}$ and below, both in the solid state and in toluene solution, and should be stored in the refrigerator. Their characterization has been limited to single-crystal X-ray diffraction and detailed NMR studies.

Solid-State and Molecular Structures. An ORTEP drawing of the molecular structure of **1**, the starting material, $W_2(OCH_2^tBu)_6(py)_2$, is shown in Figure 2 along with the atom-numbering scheme. The structure is unexceptional but serves to show how the $W_2(OCH_2^tBu)_6$ molecule picks up two "innocent" σ -donor ligands, pyridine molecules, to give the bis ligated adduct with an unbridged $W\equiv W$ bond. Selected bond distances and angles are given in Table 1. The $W-O$ and $W-N$ distances are similar to those in other $M_2(OR)_6(\text{amine})_2$ complexes, and the $W-W$ distance is typical of a $W-W$ triple bond.⁸

An ORTEP drawing of the 1,3-butadiene complex **2** is shown in Figure 3 along with the atom-numbering scheme. Selected bond distances and angles are given in Table 2.

An ORTEP drawing of the isoprene adduct **3** is given in Figure 3. In this view we are looking perpendicular to the $W-W$ bond axis and down on the μ, η^1, η^4 -isoprene ligand. Selected bond distances and angles are given in Table 3, and a summary of crystal data for the three structural determinations is given in Table 4. Com-

Table 1. Selected Bond Distances (\AA) and Bond Angles (deg) for the $W_2(OCH_2^tBu)_6(py)_2$ Molecule, **1**

A-B	distance
W(1)-W(2)	2.3340(5)
W(1)-O(3)	1.938(6)
W(1)-O(9)	1.939(4)
W(1)-O(15)	1.919(6)
W(1)-N(39)	2.268(6)
W(2)-O(21)	1.939(6)
W(2)-O(27)	1.913(6)
W(2)-O(33)	1.950(4)
W(2)-N(45)	2.267(5)
A-B-C	angle
W(2)-W(1)-O(3)	107.8(1)
W(2)-W(1)-O(9)	99.54(9)
W(2)-W(1)-O(15)	107.54(8)
W(2)-W(1)-N(39)	97.76(9)
W(1)-W(2)-O(21)	108.6(1)
W(1)-W(2)-O(27)	108.50(9)
W(1)-W(2)-O(33)	98.72(9)
W(1)-W(2)-N(45)	97.55(7)
W(1)-O(3)-C(4)	136.9(5)
W(1)-O(9)-C(10)	115.1(4)
W(1)-O(15)-C(16)	136.5(4)
W(2)-O(21)-C(22)	137.7(5)
W(2)-O(27)-C(28)	137.4(5)
W(2)-O(33)-C(34)	114.2(4)

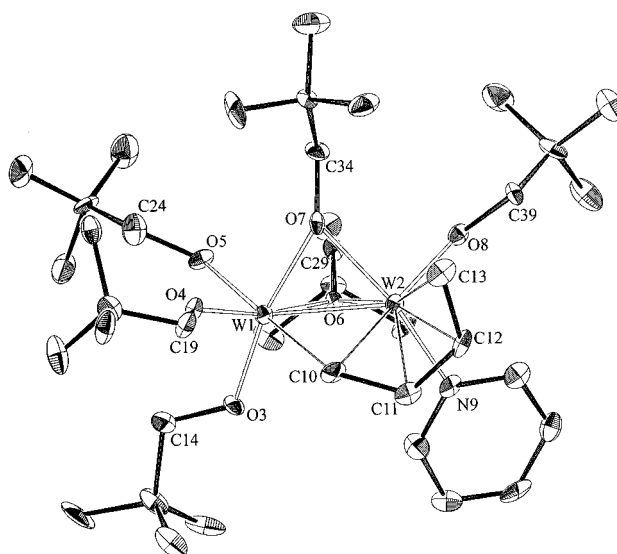
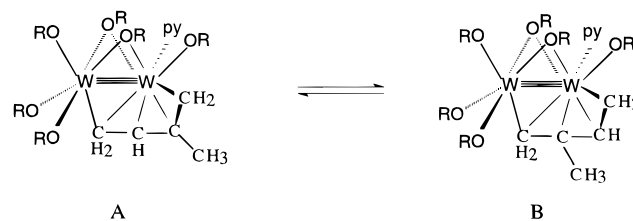


Figure 3. Structure of $W_2(OCH_2^tBu)_6(py)(\text{butadiene})$, **2**. Thermal ellipsoids are shown at the 50% probability level.

pound **3** shows a disorder of the isoprene $C-Me$ group as illustrated in the stick drawings A and B below. The dominant isomer A (70%) is the one shown in Figure 4.



The structures of both **2** and **3** have a common $W_2O_6C_4N$ core, which may be related to that of a distorted confacial bioctahedron wherein one CH_2 carbon and two oxygen atoms of $\mu-OR$ groups form the common face. In **2** one can see that one W atom, $W(1)$,

(8) Chisholm, M. H. *Polyhedron* **1983**, *2*, 681.

Table 2. Selected Bond Distances (Å) and Bond Angles (deg) for the $W_2(OCH_2^tBu)_6(py)$ (butadiene) Molecule, **2**

A–B	distance
W(1)–W(2)	2.4706(8)
W(1)–O(3)	1.909(7)
W(1)–O(4)	1.918(7)
W(1)–O(5)	1.987(7)
W(1)–O(6)	2.078(7)
W(1)–O(7)	2.083(7)
W(1)–C(10)	2.44(1)
W(2)–O(6)	2.095(7)
W(2)–O(7)	2.146(7)
W(2)–O(8)	2.049(7)
W(2)–N(9)	2.221(8)
W(2)–C(10)	2.32(1)
W(2)–C(11)	2.24(1)
W(2)–C(12)	2.28(1)
W(2)–C(13)	2.26(1)
C(10)–C(11)	1.46(2)
C(11)–C(12)	1.41(1)
A–B–C	Angles
O(3)–W(1)–O(4)	95.3(3)
O(3)–W(1)–O(5)	95.2(3)
O(3)–W(1)–O(6)	92.4(3)
O(3)–W(1)–O(7)	168.2(3)
O(3)–W(1)–C(10)	90.1(3)
O(4)–W(1)–O(5)	90.2(3)
O(4)–W(1)–O(6)	169.1(3)
O(4)–W(1)–O(7)	94.4(3)
O(4)–W(1)–C(10)	82.8(3)
O(5)–W(1)–O(6)	81.5(3)
O(5)–W(1)–O(7)	91.4(3)
O(5)–W(1)–C(10)	171.6(3)
O(6)–W(1)–O(7)	78.9(3)
O(6)–W(1)–C(10)	104.8(3)
O(7)–W(1)–C(10)	84.5(3)
C(10)–C(11)–C(12)	118.8(9)
C(11)–C(12)–C(13)	118.8(9)
W(1)–O(6)–W(2)	72.6(2)
W(1)–O(7)–W(2)	71.5(2)
W(1)–C(10)–W(2)	62.6(3)

is in a pseudo-octahedral geometry with five W–O bonds and one W–C bond of distance 2.44(1) Å. The other W atom, W(2), is coordinated to two μ -OR oxygen atoms, one terminal OR group, and a terminal pyridine in addition to the η^4 -C₄ unit. The bridging carbon atom is trans to the terminal OR group. The bonding mode of the isoprene in **3** is essentially identical.

The molecules **2** and **3** lack any element of symmetry, which does not endear them to simple MO calculations. Indeed, an EHMO calculation on $W_2(OH)_6(C_4H_6)(NH_3)$ was undertaken but was not very enlightening in terms of providing a bonding description. It is, however, evident that on going from **1**, $W_2(OCH_2^tBu)_6(py)_2$, to **2** or **3**, there is a loss of one pyridine molecule and the formation of two μ -OR bridges that accompany the substrate uptake. The order of these events is not known, but pyridine dissociation is necessary for any substrate to access the W_2 center as has been shown in reactions with ketones.⁴

The W–W distances of 2.47(1) and 2.46(1) Å in **2** and **3**, respectively, fall in the range expected for W=W bonds in a W_2^{8+} unit.⁸ This suggests that the diene is reduced and the W=W center oxidized. A simple electron-counting scheme would then require the diene to be a 2– ligand, and this can be reasoned as a metalated (μ -C, η^1,η^1) π (η^3 -allyl) moiety. The C–C distances within the coordinated 1,3-diene moiety are statistically equivalent at 1.42(2) Å, notably longer than in the free diene,

Table 3. Selected Bond Distances (Å) and Bond Angles (deg) for the $W_2(OCH_2^tBu)_6(py)$ (isoprene) Molecule, **3**

A–B	distance
W(1)–W(2)	2.4644(9)
W(2)–O(14)	2.066(8)
W(2)–O(20)	2.069(7)
W(2)–O(26)	1.890(8)
W(2)–O(32)	1.912(7)
W(2)–O(38)	1.983(8)
W(2)–C(3)	2.40(1)
W(1)–O(8)	2.011(8)
W(1)–O(14)	2.137(8)
W(1)–O(20)	2.091(8)
W(1)–N(44)	2.19(1)
W(1)–C(3)	2.31(1)
W(1)–C(4)	2.23(1)
W(1)–C(5)	2.30(1)
W(1)–C(6)	2.27(1)
C(3)–C(4)	1.47(2)
C(4)–C(5)	1.39(2)
C(5)–C(6)	1.40(2)
C(6)–C(7)	1.57(2)
A–B–C	angle
O(26)–W(2)–C(3)	90.4(4)
O(26)–W(2)–O(14)	166.3(3)
O(26)–W(2)–O(20)	92.1(3)
O(26)–W(2)–O(32)	94.9(3)
O(26)–W(2)–O(38)	95.7(3)
O(32)–W(2)–C(3)	82.4(4)
O(32)–W(2)–O(14)	96.5(3)
O(32)–W(2)–O(20)	168.8(3)
O(32)–W(2)–O(38)	90.1(3)
O(38)–W(2)–C(3)	106.3(4)
O(38)–W(2)–O(14)	91.8(3)
O(38)–W(2)–O(20)	80.6(3)
O(14)–W(2)–C(3)	83.6(4)
O(14)–W(2)–O(20)	77.8(3)
O(20)–W(2)–C(3)	106.3(4)
C(5)–C(4)–C(3)	121(1)
C(4)–C(5)–C(6)	116(1)
W(2)–O(14)–W(1)	71.8(3)
W(2)–O(20)–W(1)	72.7(3)
W(1)–C(3)–W(2)	63.1(3)

consistent with extensive reduction of the ligand. The carbon that bridges the two W atoms may be viewed as hypervalent since it is five-coordinate, being bound to two H atoms, one C atom, and the two tungsten atoms.

Solution NMR Behavior. Both compounds **2** and **3** show complex ¹H and ¹³C{¹H} NMR spectra in toluene-*d*₈ and benzene-*d*₆ because of the dynamic equilibria involving the 1:1 diene adducts and free $W_2(OCH_2^tBu)_6$, diene, and pyridine. These equilibria are temperature dependent, and above +60 °C the spectra correspond essentially to free diene, $W_2(OCH_2^tBu)_6$, and pyridine. The ¹H spectra of the 1:1 adducts are, however, clearly visible at room temperature, 500 MHz, which indicates that the equilibria, though rapid on the chemical time scale, are not so rapid as to cause line-broadening. The spectra of the 1:1 diene adducts are extremely complex because the molecules lack any element of symmetry. There are six inequivalent OCH_2^tBu groups, and each has diastereotopic methylene protons, which partially obscure the observation of the diene protons. Consequently the diene adducts involving the selectively deuterated complexes bearing $CD_2C(CH_3)_3$ ligands, hereafter referred to as CD_2^tBu , were prepared. Here for **2** we observe six ^tBu singlets of equal intensity and an a, b, c, d, e, f spin system for the coordinated butadiene. For compound **3**, the situation is further

Table 4. Summary of Crystallographic Data^a

	I	II	III
fw	1048.73	1023.72	1129.91
space group	<i>P1</i>	<i>P1</i>	<i>P2₁/n</i>
<i>a</i> , Å	11.654(2)	13.006(2)	10.520(3)
<i>b</i> , Å	18.481(4)	17.583(2)	18.475(5)
<i>c</i> , Å	11.509(2)	10.351(2)	26.692(7)
α , deg	92.58(1)	98.61(1)	90
β , deg	104.64(1)	104.13(1)	98.13(2)
γ , deg	103.38(1)	80.60(1)	90
<i>Z</i>	2	2	4
<i>V</i> , Å ³	2319.20	2249.69	5135(2)
<i>d</i> _{calc} , g cm ⁻³	1.502	1.511	1.461
cryst size, mm	0.08 × 0.16 × 0.32	0.30 × 0.15 × 0.10	0.32 × 0.16 × 0.12
cryst color	dark red	colorless	purple
linear abs coeff, cm ⁻¹	50.027	52.572	46.132
temp, °C	-172	-173	-165
takeoff angle, deg	2.0	2.0	3.0
scan speed, deg/min	8.0	6.0	8.0
scan width, deg	2.1	2.0	2.4
2 θ range, deg	6–45	6–45	6–45
data collected	12 476	10 405	13 873
unique data	6108	8858	6685
unique data with <i>F</i> > 3 σ (<i>F</i>)	4776	5487 ^b	4474 ^c
<i>R</i> (<i>F</i>)	0.0373	0.0403	0.0471
<i>R</i> _w (<i>F</i>)	0.0366	0.0424	0.0945 ^d
goodness of fit	1.235	0.970	1.071
max Δ / σ	0.63	0.02	0.03

^a I, W₂(OCH₂^tBu)₆(py)₂; II, W₂(OCH₂^tBu)₆(py)(butadiene); III, W₂(OCH₂^tBu)₆(py)(isoprene). ^b Number with *F* > 2.33 σ (*F*). ^c Number with *F* > 4 σ (*F*). ^d *R*_w(*F*²) for all data.

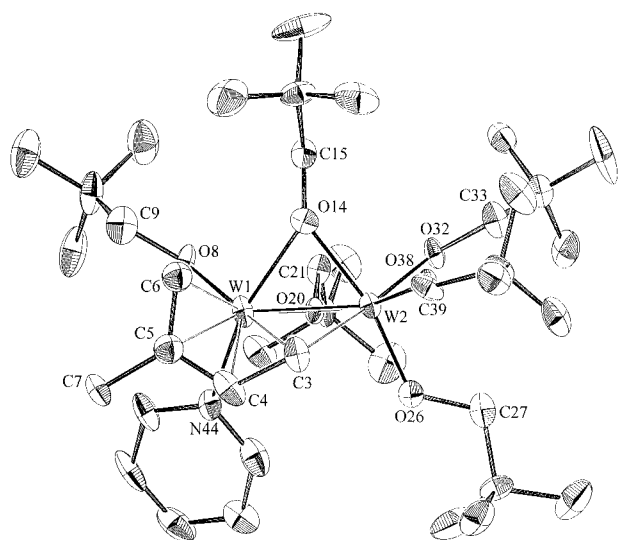


Figure 4. Structure of W₂(OCH₂^tBu)₆(py)(isoprene), **3**, isomer A (see text). Thermal ellipsoids are shown at the 50% probability level.

complicated by the appearance of two isomers, which at room temperature are in near equal concentration. For **3**, we observe 12 ^tBu signals assignable to these isomers.

We have interrogated the solution behavior of **2** and **3** by a variety of variable-temperature NMR spectroscopic studies including COSY, HETCOR, phase-sensitive HETCOR, and spin magnetization transfer. From these studies we can make the following conclusions.

1. The methylene carbon that bridges the two tungsten atoms shows the most upfield shift of the diene carbons. This bridging carbon shows coupling to two tungsten atoms (*J*_{W-¹³C} ≈ 35 Hz), and the *J*_{C-¹H}

values associated with this carbon are the smallest and fall in the range 124–140 Hz. (The other diene carbon atoms do not show any resolvable coupling to ¹⁸³W, *I* = ¹/₂, 14.5% nat. abund.)

2. The two isomers of **3** are in equilibrium. From an analysis of the NMR data, we conclude that the one having the structure shown in Figure 4 (isomer A) is somewhat favored at lower temperatures. (The crystal structure revealed a 70:30 mixture with respect to the isoprene–Me group.) The variable-temperature NMR data indicate that while isomer A is enthalpically favored, isomer B is entropically favored. We estimate that for the equilibrium A ⇌ B the thermodynamic data are $\Delta H^\circ = +2.4(1)$ kcal/mol and $\Delta S^\circ = +4(1)$ eu.

3. Spin magnetization transfer experiments (irradiation of the isoprene–Me protons involving the coordinated and free ligand) indicate that the two isomers interconvert by a dissociative process. A point worthy of mention is that when one irradiates the free isoprene–Me protons, the difference spectrum associated with exchange with the bound ligand is apparently less than when the experiment is carried out in the reverse sense. This is because of facile energy loss (transfer) by NOE to the other protons of the free isoprene.

A ¹H NMR spectrum of W₂(OCD₂^tBu)₆(CH₂CHCMe–CH₂)(py) in toluene-*d*₈ solution is shown in Figure 5. This clearly shows the 12 ¹H signals assignable to the isoprene protons of the two isomers present in solution together with free isoprene. There are also the signals of protio toluene which arise because crystallization of **3** from toluene gives a toluene solvate. A COSY spectrum is shown in Figure 6 and reveals the connectivity of the spin systems within the bound isoprene ligands of each isomer. The HETCOR spectrum is shown in Figure 7. Full NMR data are given in the Experimental Section.

Interpretation of 2D NMR Spectra. The COSY spectrum of W₂(OCD₂^tBu)₆(py)(μ -isoprene) (Figure 6) shows the proton–proton coupling of the isoprene adduct. The isoprene adduct of each isomer should exhibit three spin systems. One spin system consists of the two methylene protons and an adjacent methyne proton (a, b, c, and f, g, h); a second system consists of the other methylene protons (d, e and i, j); the last spin system consists of the methyl protons (Me, Me'), which are not coupled to any other protons. For reference, the a, b, c, d, e spin system is assigned to the peaks of the isomer whose relative concentration increases at lower temperatures.

The HETCOR spectrum of W₂(OCD₂^tBu)₆(py)(μ -isoprene) (Figure 7) shows the coupling between the carbon atoms and the protons of each isoprene adduct. Furthermore, the spectrum shown is phase-sensitive, and only the resonances arising from –CH₂ groups are observed. Four pairs of signals resulting from one carbon resonance and two inequivalent proton resonances are visible. The resonances can be assigned to the two isomers A and B using the results of the variable-temperature NMR experiments as well as the COSY experiment. Isomer A is assigned to the resonances of the isomer whose relative concentration increases at lower temperatures.

As the carbon peaks centered around 44 ppm show coupling to two tungsten atoms (*J*_{W-¹³C} ≈ 35 Hz, *I* =

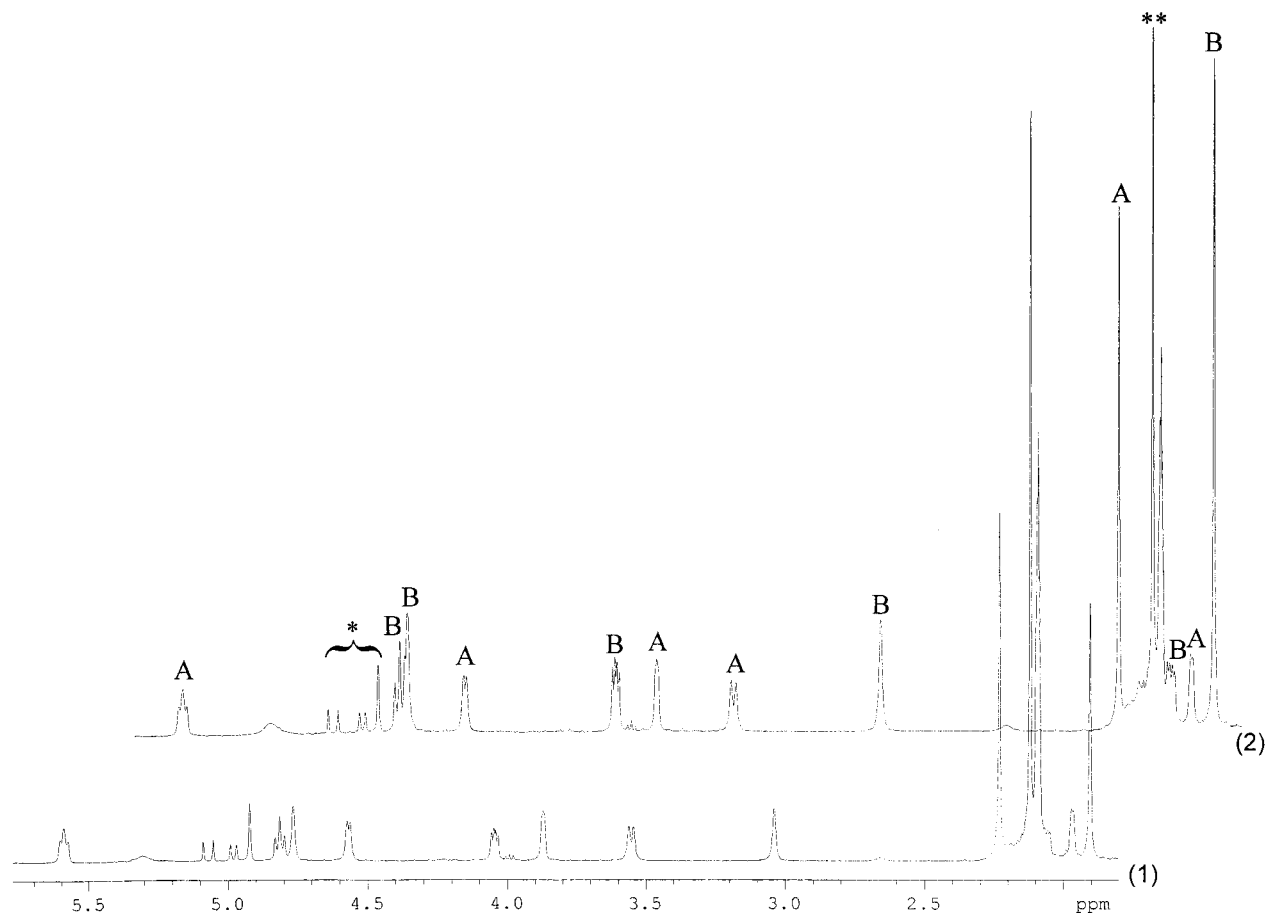


Figure 5. Variable-temperature ^1H NMR spectra of $\text{W}_2(\text{OCD}_2^t\text{Bu})_6(\text{py})(\mu\text{-isoprene})$ recorded at 500 MHz in toluene- d_8 (1) at -15°C , (2) at 20°C . The signals denoted by * correspond to the methylene signals of free isoprene. The signals denoted by ** correspond to $\text{C}_6\text{H}_5\text{CH}_3$ and $\text{C}_6\text{D}_5\text{CD}_2\text{H}$.

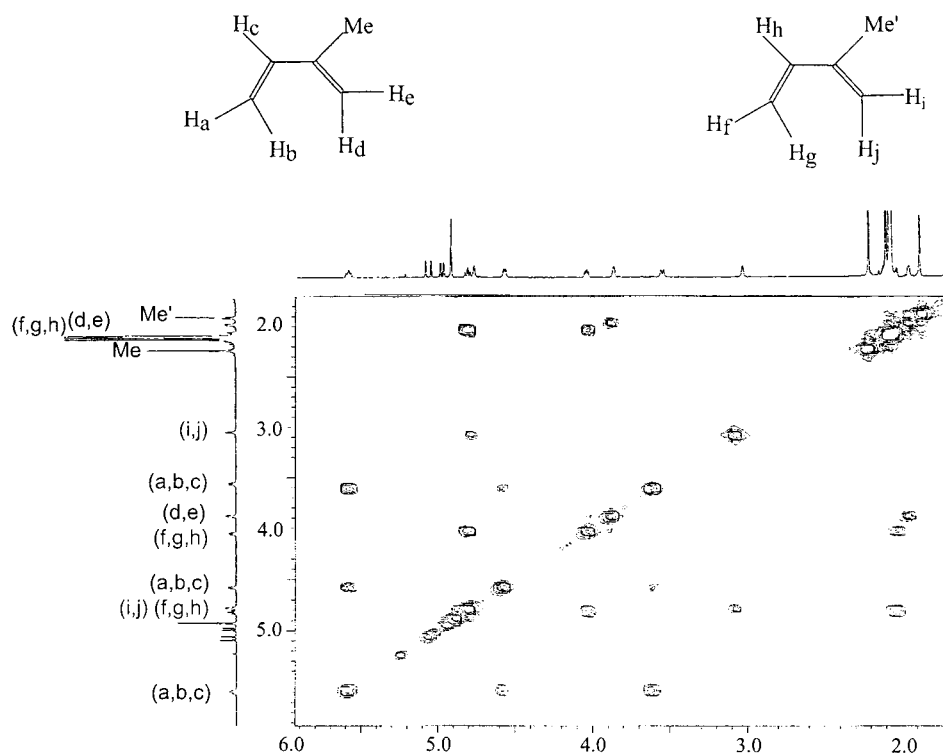


Figure 6. ^1H COSY of $\text{W}_2(\text{OCD}_2^t\text{Bu})_6(\text{py})(\mu\text{-isoprene})$ recorded at 500 MHz in toluene- d_8 showing the ^1H - ^1H spin connectivity in the isomers A and B.

30%), these resonances correspond to the bridging carbon atom. Returning to the results from the COSY

experiment, it is noted that the bridging carbon atom in isomer A belongs to a three-proton spin system, while

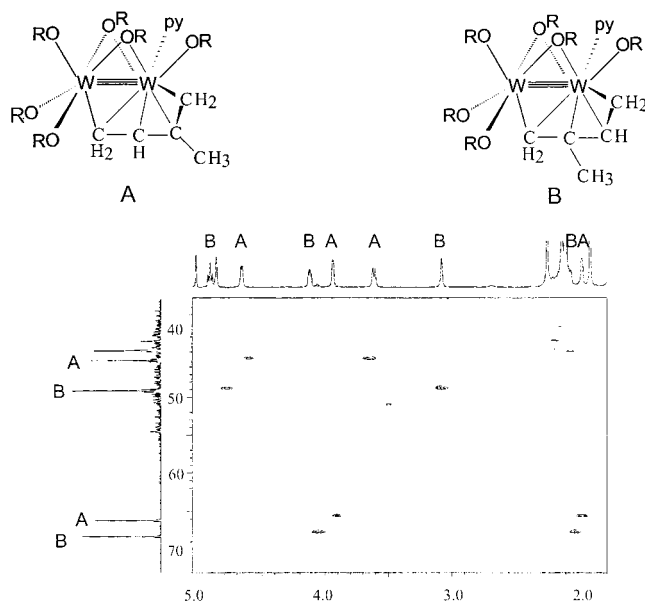


Figure 7. Phase-sensitive HETCOR of $W_2(OCH_2^tBu)_6(py)(\mu\text{-isoprene})$ obtained in benzene- d_6 at 20 °C, 72 h, recorded on a UNITY plus-400 showing the 1H - ^{13}C connectivity for the methylene resonances of isomer A and isomer B.

the bridging carbon atom in isomer B belongs to a two-proton spin system. Thus the combination of 2D NMR experiments allows us to identify the structures of isomers A and B as shown in Figure 7.

Comparisons with Other Diene Structures. The structures of a wide variety of 1,3-diene adducts have been determined in organometallic chemistry, and various bonding modes have been seen. These are represented schematically in Figure 8. Thus, it appears that the μ, η^1, η^4 - C_4 mode of bonding observed in compounds **2** and **3** has not been seen before. The coordination of the μ, η^1 -carbon atom is "hypervalent" in that the carbon atom forms bonds to two hydrogen atoms, one carbon atom, and two metal atoms. Such coordination is typical of bridging alkyl ligands as in $Al_2(\mu\text{-}CH_3)_2(CH_3)_4$,⁹ but continues to attract attention in the current literature.¹⁰ What is perhaps remarkable given the structures seen for **2** and **3** is that the diene fragment is readily, but reversibly, released in solution. This observation led us to examine the possibility of catalytic activity with respect to hydrogenation.

Hydrogenation. Although we have been able to observe adduct formation only for 1,3-butadiene and isoprene, we have found that 1,3-acyclic dienes and $W_2(OCH_2^tBu)_6(py)_2$ react in hydrocarbons in the presence of H_2 (1–4 atm) to give 3-enes. Furthermore when 1,3-butadiene or isoprene is allowed to react with D_2 , we have observed by NMR spectroscopy the formation of $CH_2DCHDCH=CH_2$ and $CH_2C(Me)CHDCH_2D$. The stereospecific 1,2-addition is of interest since commonly if a metal hydride is employed, one sees scrambling and formation of 2-enes as a result of π -allyl formation. Indeed, reactions between $W_2(H)(OR)_7$ compounds and 1,3-dienes and H_2 in hydrocarbons give mixtures of

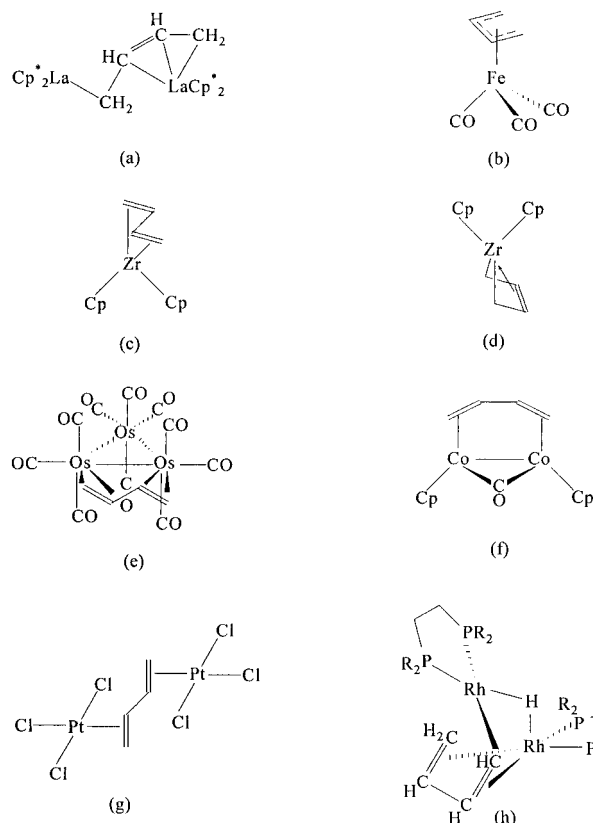


Figure 8. Structural representations of previously observed binding modes of 1,3-dienes to metal centers: (a) $[Cp^*_2La]_2(\mu\text{-}\eta^1, \eta^3\text{-}C_4H_6)$,¹⁷ (b) $Fe(CO)_3(C_4H_6)$,¹⁸ (c) $Cp_2Zr(s\text{-}trans\text{-}C_4H_6)$,¹⁹ (d) $Cp_2Zr(s\text{-}cis\text{-}C_4H_6)$,²⁰ (e) $Os_3(CO)_{10}(s\text{-}trans\text{-}C_4H_6)$,²¹ (f) $Cp_2Co_2(\mu\text{-}\eta^4\text{-}syn\text{-}C_4H_6)(\mu\text{-}CO)$,²² (g) $[Pt_2Cl_6(C_4H_6)]^{-2}$,²³ (h) $[(^iPr_2P(CH_2)_2P^iPr_2)Rh]_2(\mu\text{-}H)(\mu\text{-}\eta^4, \eta^1\text{-}C_4H_5)$.²⁴

products.¹¹ Since we have not observed any direct reaction between $W_2(OR)_6$ compounds and H_2 in hydrocarbon solvents, it seems plausible that the initial reaction involves uptake of the diene at the metal center followed by a hydrogenolysis reaction. The nature of the latter is clearly speculative and could involve a σ -bond metathesis followed by a rapid C–H bond reductive elimination.

Given the unusual coordination geometry of the W_2 -diene moiety, one might well ask which C_2 unit of the C_4 bond fragment is hydrogenated. The most activated C_2 moiety would involve the carbon that is bridging the W_2 center, while the least activated is the η^2 - C_2 unit bonded to $W(2)$ in Figure 3 or $W(1)$ in Figure 4. We have given considerable thought to this matter, but it may prove irrelevant as we have found that isolated cis-olefins, particularly those within rings, are capable of being hydrogenated. Rather interestingly no 1:1 cis-olefin adducts have been detected, and ethylene, which reversibly forms a bis-ethylene adduct, $W_2(OCH_2^tBu)_6(\eta^2\text{-}C_2H_4)_2$, is *not* hydrogenated. Collectively these observations lead us to propose that it is a transient $W_2(OCH_2^tBu)_6(\eta^2\text{-}ene)$ complex that reacts with H_2 and that in the case of 1,3-cis-dienes the chelate effect merely facilitates the μ, η^1, η^4 -binding mode seen in **2** and **3**. The uptake of the diene in the formation of **2** and **3** requires a considerable degree of rearrangement of the

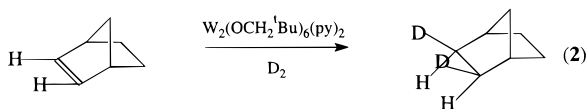
(9) Lewis, P. H.; Rundle, R. E. *J. Chem. Phys.* **1953**, *21*, 986.

(10) A recent example, the (alkenyl)zirconocene compound $(MeCp)_2Zr(\mu\text{-}Cl)(\mu\text{-}CH_2CH\text{-}n\text{-}butyl)Zr(MeCp)_2^+$, is found in: Schottek, J.; Röttger, D.; Erker, G.; Fröhlich, R. *J. Am. Chem. Soc.* **1998**, *120*, 5264.

(11) Barry, J. T.; Chacon, S. T.; Chisholm, M. H.; Huffman, J. C.; Streib, W. E. *J. Am. Chem. Soc.* **1995**, *117*, 1974.

$W_2(OR)_6$ moiety, and this clearly does not occur in a single step. Rather we propose there is an initial reaction between $W_2(OCH_2^tBu)_6$ and the α -olefin which is then followed by coordination of the conjugated double bond. We have seen similar behavior in the reactions between $W_2(OCH_2^tBu)_6$ and α,β -unsaturated aldehydes and ketones, which may give 1,2- or 1,4-addition products depending upon the steric encumbrance of the organic molecule which is coordinating to the W_2^{6+} center. See Figure 1.

While we have shown that hydrogenation occurs in a 1,2-manner, we have not been able to elucidate the stereochemistry of this addition for 1,3-butadiene or isoprene. However, by use of norbornene as a cis-ene we have found that the addition of D_2 occurs in the cis-manner shown in eq 2. Specifically the D_2 addition



occurs to the least sterically encumbered face of the C–C double bond to give the endo- d_2 norbornane. In a competition experiment norbornene was allowed to react with an excess of a 50:50 mixture of H_2/D_2 in benzene, and the formation of norbornane was monitored with time at 25 °C. From this reaction we obtain a k_H/k_D ratio of 1.7, which is small but significant. However, an interpretation of this k_H/k_D value is subject to various possible scenarios in terms of the reaction sequence.¹² It does, however, implicate that C–H and/or W–H bond forming steps contribute to the overall rate expression for k_{obs} .

In a separate competition experiment, we studied the hydrogenation of equimolar amounts of isoprene and norbornene in cyclohexane- d_{12} and followed the disappearance of the two substrates with respect to an internal standard of Me_4Si . Within the limits of experimental error the two were hydrogenated at the same rate, despite the observed preferential coordination of isoprene. This would seem to be yet another support for the view that the species seen by 1H NMR in a catalytic system are all too often irrelevant to the reactive intermediates in the catalytic cycle.¹³

Concluding Remarks

The reversible binding of 1,3-butadiene and isoprene to the W_2^{6+} center supported by six neopentoxide ligands provides yet another example of the flexibility of the $W_2(OR)_6$ template in organometallic chemistry.

(12) While the elimination of R–H from d^0 metal centers via a σ -bond metathesis mechanism has not been observed to give a measurable kinetic isotope effect, the oxidative addition and reductive elimination of H_2 from tungsten have been observed to give normal kinetic isotope effects. For the reductive elimination of R–H from metal centers, both inverse and normal kinetic isotope effects have been observed. It has been proposed that the inverse kinetic isotope effect is due to the presence of a preequilibrium step or an alkyl-hydride complex, while the normal kinetic isotope effect arises from simple, concerted reductive elimination of R–H. For leading references see: (a) Crellin, K. C.; Geribaldi, S.; Widmer, M.; Beauchamp, J. L. *Organometallics* **1995**, *14*, 4366. (b) Rabinovich, D.; Parkin, G. *J. Am. Chem. Soc.* **1993**, *115*, 353. (c) Gould, G. L.; Heinekey, D. M. *J. Am. Chem. Soc.* **1989**, *111*, 5502. (d) Deutsch, P. P.; Eisenberg, R. *Organometallics* **1990**, *9*, 709.

(13) Halpern, J. *Science* **1982**, *217*, 401.

Steric and electronic factors are obviously important, as no such adducts are seen for $Mo_2(OCH_2^tBu)_6$ or for $W_2(OR)_6$ compounds where $R = ^tBu$ or iPr . It is interesting to note that this mode of coordination has not been seen before. See Figure 8. The reactions involving H_2 to give 3-enes, though very slow in the present cases (ca. 1 turnover per mole h, 25 °C, 1 atm), suggest that with a judicious selection of RO and reaction conditions this could become a useful reaction. Further studies along these lines are planned. Finally, it is worth commenting on the question we originally posed. Will metal–metal triple bonds enter into Diels–Alder type reactions? Since this is the first and only report of the addition of a 1,3-diene to a $M\equiv M$ bond, it is clearly premature to rule out the possibility of the reaction shown in eq 3. However, one thing that is clear from



the present study is that the addition of the 1,3-diene to give the $\mu-\eta^1,\eta^4$ -adduct maximizes metal ligand bonding in a way that a simple Diels–Alder addition of the type shown in eq 3 does not. If other addition reactions between $M\equiv M$ bonds and 1,3-dienes are observed, we expect to see a similar preference for maximizing metal–ligand bonding.

Experimental Section

Reagent and General Techniques. General procedures and the preparation of $W_2(OCH_2^tBu)_6(py)_2$ have been described.¹⁴ Preparation of the partially deuterated compound $W_2(OCd_2C(CH_3)_3)_6(C_5H_5N)_2$ was carried out using the deuterated alcohol $HOCD_2C(CH_3)_3$, as prepared previously.¹⁵

All preparations were carried out in an inert atmosphere using standard Schlenk and drybox techniques. Hydrocarbon solvents and ether were dried and distilled from sodium diphenyl ketyl and stored over 4 Å molecular sieves. Pyridine was washed with a sodium hydroxide solution, dried and distilled from calcium oxide, and stored over 4 Å molecular sieves. Methyl pivalate was dried and distilled from P_2O_5 and stored over 4 Å molecular sieves. Isoprene was degassed with dry nitrogen and stored over 3 Å molecular sieves. NMR solvents (benzene- d_6 and toluene- d_8) were dried over 4 Å molecular sieves and degassed with dry nitrogen. Neopentanol and lithium aluminum deuteride were purchased from Aldrich and used without further purification.

1H NMR spectra were recorded on a Gemini-300 300 MHz spectrometer, a UNITYplus-400 400 MHz spectrometer, or a UNITYplus-500 500 MHz spectrometer in dry and oxygen-free benzene- d_6 and toluene- d_8 . ^{13}C NMR spectra were recorded on the Gemini-300 300 MHz spectrometer or on the UNITYplus-400 400 MHz spectrometer at 75 or 100 MHz, respectively. All 1H NMR chemical shifts are in ppm relative to the C_6D_5H singlet of benzene- d_6 set at δ 7.15 or the methyl protio impurity in toluene- d_8 set at δ 2.09. ^{13}C NMR chemical shifts are in ppm relative to the C_6D_6 triplet of benzene- d_6 set at δ 128.0. Values of coupling constants (J) are reported in hertz.

$W_2(OCH_2^tBu)_6(py)$ (butadiene) (2). $W_2(OCH_2^tBu)_6(py)_2$ (0.02 g, 0.013 mmol) was dissolved in toluene- d_8 in a J. Young tube. The sample was frozen and evacuated, and 1,3-butadiene (14 Torr, 0.05 mmol) was added from a calibrated gas manifold.

(14) Akiyama, M.; Chisholm, M. H.; Cotton, F. A.; Extine, M. W.; Haitko, D. A.; Little, D.; Fanwick, P. E. *Inorg. Chem.* **1979**, *18*, 2266.

(15) Chu, K. S.; Negrete, G. R.; Konopelski, J. P.; Lakner, F. J.; Woo, N.-T.; Olmstead, M. M. *J. Am. Chem. Soc.* **1992**, *114*, 1810.

The tube was warmed to room temperature and turned dark blue in approximately 10 min. After the color change had been observed, the NMR spectra were recorded. Preparations of **2** using the same general procedure resulted in an approximately 60% yield of X-ray quality crystals. ^1H NMR (300 MHz, 22 °C, toluene- d_6): δ = py, 9.1 (br, 2H), 7.10 (br, 1H), 6.80 (br, 2H); C_4H_6 : 5.79(m, 1H), 5.25 (m, 1H), 4.82 (m, 1H), 4.07 (m, 1H), 3.47 (m, 1H), 1.56 (m, 1H); OCH_2Bu , 5.5–3.5 (overlapping d, 12H); $\text{OCH}_2\text{C}(\text{CH}_3)_3$, 1.34 (s, 9H), 1.15 (s, 9h), 1.34–1.01 (br overlapping s, 27H), 0.61 (s, 9H). $^{13}\text{C}\{^1\text{H}\}$ NMR (126 MHz, 22 °C, toluene- d_6): δ = py, 150.3, 130.2, 122.1; C_4H_6 , 111.8, 102.9, 66.2, 44.8; OCH_2Bu , 77.8–62.1 (overlapping s); $\text{OCH}_2\text{C}(\text{CH}_3)_3$, 38.3, 35.5, 33.1, 29.6, 28.2, 22.4.

^{13}C NMR (126 MHz, 22 °C, toluene- d_6): δ = C_4H_6 , 111.8 (d, $J_{\text{C-H}} = 174$), 102.9 (d, $J_{\text{C-H}} = 164$), 66.2 (t, $J_{\text{C-H}} = 157$), $J_{\text{is}^3\text{W}} = 24$, $I = 14\%$), 44.8 (t, $J_{\text{C-H}} = 149$, 124, $J_{\text{is}^3\text{W-H}} = 34$ Hz, $I = 25\%$).

$\text{W}_2(\text{OCD}_2\text{Bu})_6(\text{py})(\mu\text{-isoprene})$ (2**).** To a deep red solution of $\text{W}_2(\text{OCD}_2\text{Bu})_6(\text{py})_2$ (474 mg, 0.447 mmol) in toluene (20 mL) was added isoprene (5 mL, 50.0 mmol). The color of the solution became purple. The solution was allowed to stir at room temperature for 12 h, at which time the solvent volume was reduced and the flask cooled to -20 °C. After 6 days, purple crystals of $\text{W}_2(\text{OCD}_2\text{Bu})_6(\text{py})(\mu\text{-isoprene})$ were isolated by removing the supernatant liquid via cannula and were dried under vacuum (75.0 mg, 0.0664 mmol, 15.0% yield). ^1H NMR (500 MHz, toluene- d_6 , -15 °C): δ = 9.55 (b), 8.63 (d, $J_{\text{HH}} = 6$), 8.44 (d, $J_{\text{HH}} = 5.5$), 7.60 (d, $J_{\text{HH}} = 5$), 7.15 (d, $J_{\text{HH}} = 5.5$), 6.83 (m), 6.80 (b), 6.62 (t, $J_{\text{HH}} = 7.5$), 6.52 (t, $J_{\text{HH}} = 7$), 5.54 (7, $J_{\text{HH}} = 7$, B), 4.76 (t, $J_{\text{HH}} = 8$, A), 4.71 (s, A), 4.52 (d, $J_{\text{HH}} = 5.5$, B), 3.99 (s, A), 3.80 (m, B), 3.50 (d, $J_{\text{HH}} = 8.5$, B), 2.99 (s, A), 2.18 (s, B), 2.04 (m), 2.00 (m, A), 1.92 (d, $J_{\text{HH}} = 3$, B), 1.85 (s, A), 1.60 (b), 1.35 (m), 1.18 (m), 1.12 (s), 1.05 (m), 1.01 (m), 0.66 (s), 0.54 (s). $^{13}\text{C}\{^1\text{H}\}$ NMR (100.61 MHz, C_6D_6 , 20 °C): δ = 157.78, 157.23, 153.80, 152.84, 150.94, 138.65, 137.87, 123.22, 123.05, 116.22, 115.49, 109.31, 102.91, 80.14, 67.78, 65.69, 48.83, 44.83, 43.59, 36.19, 35.48, 35.40, 35.20, 35.13, 34.45, 34.38, 33.83, 33.77, 33.57, 28.33, 28.24, 28.11, 27.94, 27.62, 27.33, 27.25, 25.17, 22.78.

Determination of ΔH^\ddagger and ΔS^\ddagger Values. A solution of **3** in toluene- d_6 was studied using variable-temperature NMR spectroscopy. The solution was gradually warmed from -15 °C to 20 °C in 5 °C increments and was allowed to come to equilibrium after each temperature change. The relative amounts of isomers A and B were determined by integration. An Eyring plot was constructed to determine the values of ΔH^\ddagger and ΔS^\ddagger . While the statistical treatment of the data gives $\Delta H^\ddagger = 2.44(1)$ kcal/mol and $\Delta S^\ddagger = 4.4(1)$ eu, we report $\Delta H^\ddagger = 2.4(1)$ kcal/mol and $\Delta S^\ddagger = 4(1)$ eu to account for errors in temperature and integration.

Procedure for Hydrogenation/Deuteration Reactions. In a typical experiment, $\text{W}_2(\text{OCD}_2\text{Bu})_6(\text{py})_2$ (0.025 g, 0.024

mmol) was placed in an NMR tube equipped with a Rototite cap, and benzene- d_6 (0.30 mL) was added under a nitrogen atmosphere. Olefin (50 equiv) was added under a nitrogen atmosphere, and the solution was frozen and evacuated. An excess (3 atm) of H_2 , D_2 , or a 1:1 mixture of H_2 and D_2 was then added using a calibrated vacuum manifold. The tube was closed, and the solution was warmed to room temperature. The ^1H NMR spectra were monitored over the next two weeks, and the product signals were observed and integrated. In the reactions involving norbornene that determined the stereochemistry of the added D_2 and the presence of an isotope effect, the organic components of the reaction mixture were separated from the catalyst by vacuum transfer. All manipulations were undertaken using standard inert atmosphere techniques. The norbornane signals were integrated; deconvolution from overlapping norbornene signals was achieved by integrating non-overlapping olefin and alkane peaks and making the appropriate corrections.

Crystallographic Studies

General operating facilities and listings of programs have been given previously.¹⁶ A summary of crystal data for the three compounds studied in this work is given in Table 4. Full details have been submitted as CIF files to the Cambridge Crystallographic Data Center.

Acknowledgment. We thank the National Science Foundation and the Department of Energy, Office of Basic Energy Sciences, Chemistry Division, for financial support.

Supporting Information Available: Tables of bond distances and angles for **1–3** and ^1H and $^{13}\text{C}\{^1\text{H}\}$ NMR spectra for **2** and **3**. This material is available free of charge via the Internet at <http://pubs.acs.org>.

OM990059I

(16) (a) Huffman, J. C.; Lewis, L. N.; Caulton, K. G. *Inorg. Chem.* **1980**, *19*, 2755. (b) Chisholm, M. H.; Folting, K.; Huffman, J. C.; Kirkpatrick, C. C. *Inorg. Chem.* **1984**, *23*, 1021.

(17) Scholz, A.; Smola, A.; Scholz, J.; Loebel, J.; Schumann, H.; Thiele, K.-H. *Angew. Chem., Int. Ed. Engl.* **1991**, *30*, 435.

(18) Mills, O. S.; Robinson, G. *Acta Crystallogr.* **1963**, *16*, 758.

(19) Erker, G.; Wicher, J.; Engel, K.; Rosenfeldt, F.; Dietrich, W.; Krüger, C. *J. Am. Chem. Soc.* **1980**, *102*, 6346.

(20) Benn, R.; Grodny, H.; Erker, G.; Aul, R.; Nolte, R. *Organometallics* **1990**, *9*, 2493.

(21) Tachikawa, M.; Shapley, J. R.; Haltiwanger, R. C.; Pierpont, C. G. *J. Am. Chem. Soc.* **1976**, *98*, 4651.

(22) King, J. A., Jr.; Vollhardt, K. P. C. *Organometallics* **1983**, *2*, 684.

(23) Adam, V. C.; Jarvis, J. A. J.; Kilbourn, B. T.; Owson, P. G. *J. Chem. Soc., Chem. Commun.* **1971**, 467.

(24) Fryzuk, M. D.; Piers, W. E.; Rettig, S. J.; Einstein, F. W. B.; Jones, T.; Albright, T. A. *J. Am. Chem. Soc.* **1989**, *111*, 5709.